

Experimental and theoretical study of the reaction of OH radical with sabinene

N. Carrasco,^a M. T. Rayez,^{*b} J. C. Rayez^b and J. F. Doussin^a

Received 28th March 2006, Accepted 1st June 2006

First published as an Advance Article on the web 13th June 2006

DOI: 10.1039/b604489a

The gas phase sabinene + OH reaction is studied both experimentally and theoretically. Product yields from the reaction of sabinene with OH radicals have been measured in the absence of NO_x in the UCC chamber (Cork, Ireland) and in the presence of NO_x in the LISA chamber. Three primary carbonyl compounds were observed and quantified: acetone in [(24 ± 6)%], formaldehyde in [(25 ± 6)%] and sabinaketone in [(20 ± 6)%]. The simultaneous quantification of these compounds is one of the major results of this work. The mechanism of product formation for this reaction has been studied using the quantum chemical DFT-B3LYP (6-31G(d,p) method. According to these calculations, the H-atom abstraction channel from sabinene by OH in the initial oxidation step may be taken into account to explain the acetone production. Sabinaketone and formaldehyde are mainly products of the addition channels of OH on the -C=CH₂ double bond of sabinene. This is the first theoretical work on the title reaction.

Introduction

Large quantities of biogenic volatile organic compounds (BVOCs) are emitted by terrestrial and marine sources. The world-wide emission rate of non-methane biogenic volatile organic compounds is estimated to be 1150 TgC year⁻¹ (Guenther *et al.*¹) and of the estimated 84 TgC year⁻¹ emitted in the US, 20% are monoterpene compounds (C₁₀H₁₆).² Sabinene is a monoterpene of which the reactivity has been rarely studied. There is only one piece of kinetic data available about its reaction with OH radicals³ ($k = 1.17 \times 10^{-10}$ molecule⁻¹ cm³ s⁻¹). However, this compound has been reported to be abundantly emitted by several common tree species in Europe. Thus, Tollsten and Müller,⁴ Owen *et al.*,⁵ Street *et al.*⁶ and Hakola *et al.*⁷ have identified sabinene as a major emission from *Fagus sylvatica*, *Quercus ilex* and *Betula pendula*. Therefore, its high reactivity with OH (lifetime 1.5 h for an average OH radical concentration of 1.5×10^6 molecule cm⁻³, ref. 3) and its potentially very abundant emissions suggest that sabinene is likely to play a significant role in the chemistry of the rural troposphere.

The mechanism of the gas phase degradation of sabinene with OH radicals has been studied previously by Reissel *et al.*,⁸ Hakola *et al.*⁹ and Arey *et al.*¹⁰ Reissel *et al.*⁸ have observed the production of acetone with a yield of 0.19 ± 0.03 . This result is of atmospheric importance since it has been shown that the photolysis of acetone is a significant source of HOx radicals in the upper troposphere (Jaeglé *et al.*,¹¹ Jacob *et al.*¹²). In addition, Hakola *et al.*⁹ and Arey *et al.*¹⁰ have identified another major product, sabinaketone with a yield of

0.17. Since sabinaketone is not commercially available, this yield was determined in the absence of an authentic standard, thanks to the approximation of the GC-FID response factor using the effective carbon number concept.

In this work, the reaction of sabinene with OH radicals has been experimentally studied with and without the presence of NO_x. In addition, sabinaketone has been synthesized and used to quantify its yield from the reaction sabinene + OH. In the second part of this work, a theoretical study of the mechanisms of the oxidation of sabinene by OH is performed, explaining the formation of the primary products observed experimentally.

Experimental

Smog chambers

Experiments were carried out using two different atmospheric simulation chambers, at LISA (Créteil, France) and at University College Cork (UCC, Ireland). Both chambers have been described in detail elsewhere (Doussin *et al.*,¹³ Thuener *et al.*¹⁴) and only brief details are provided here.

The LISA chamber is a 977 L cylindrical Pyrex evacuable reactor, equipped with a multiple-reflection optical system coupled to a Bomem DA8-ME FTIR spectrometer.¹³ Between each experiment, the simulation chamber was conditioned by lowering the pressure to 10⁻³ mbar. Then, the chamber was filled with synthetic air (80% N₂, 20% O₂) at atmospheric pressure and the temperature was kept at 293 ± 2 K during all the experiments. The reactor is surrounded by 40 visible lamps (Philips TL03 40W, $\lambda_{\text{max}} = 420$ nm).

The hydroxyl radical reactions were performed using the photolysis (at 420 nm) of HONO. The initial reactant concentrations (in molecule cm⁻³) were as follows; [HONO] = 25×10^{13} , [sabinene] = 5×10^{13} . During the reactions, the contents of the chamber were continuously monitored by

^a Laboratoire Interuniversitaire des Systèmes Atmosphériques, UMR 7583 CNRS/Université Paris 7/Université Paris, 1261 av du Général de Gaulle, 94010 Créteil Cédex, France

^b Laboratoire de Physicochimie Moléculaire, UMR 5803 CNRS/Université Bordeaux 1, 33405 Talence Cedex, France. E-mail: mt.rayez@lpcm.u-bordeaux1.fr; Fax: (33) 5 40 00 66 45

FTIR spectroscopy using a path length of 156 m. Infrared spectra were obtained at a resolution of 0.5 cm^{-1} using a MCT detector and derived from the co-addition of 200 scans collected over 5 min.

The chamber at UCC is a cylinder made of FEP (fluorine-ethene-propene) foil (4.1 m long, 1.1 m diameter and 0.127 mm thickness) with a volume of 3.91 m^3 . It is operated at $295 \pm 2\text{ K}$ using purified dry air at 0.1–1 mbar above atmospheric pressure. The chamber is equipped with a multiple reflection optical arrangement coupled to an FTIR spectrometer (BioRad Excalibur) for chemical analysis by *in situ* FTIR spectroscopy. The chamber is surrounded by 18 Philips TUV (40 W) lamps with an emission maximum at 254 nm and 18 Philips TL05 (40 W) lamps with an emission maximum at 360 nm. Between experiments the chamber is cleaned by flushing with the purified air at a flow rate of $0.15\text{ m}^3\text{ min}^{-1}$ for a minimum of 4 h.

The hydroxyl radical reactions were performed in the absence of NO using the photolysis of hydrogen peroxide (by the Philips TUV lamps) as the radical source. The initial reactant concentrations (in molecule cm^{-3}) were as follows; $[\text{H}_2\text{O}_2] = 2.5 \times 10^{13}$, $[\text{sabinene}] = 5.0 \times 10^{13}$. During the reactions, the contents of the chamber were continuously monitored by FTIR spectroscopy using a path length of $(229.6 \pm 0.6)\text{ m}$. Infrared spectra were obtained at a resolution of 1 cm^{-1} using a narrow-band MCT detector and derived from the co-addition of 200 scans collected over 4 min.

FTIR spectroscopy

Quantitative analysis was performed by subtraction of calibrated reference spectra of known compounds and subsequent integration of selected absorption bands for sabinene and the reaction products. The integrated band intensities (IBI) of spectral regions used during the subtraction procedures are given in Table 1.

Chemicals. Chemicals were obtained from the following sources and used without further purification: sabinene (Interchim, >99%), H_2O_2 (Aldrich, 30%). HONO was synthesised from the dropwise addition of sulfuric acid to a diluted NaNO_2 solution (Taylor *et al.*¹⁵). Sabinaketone was previously synthesized by sabinene ozonolysis in the liquid phase (GCMS, >95%). The method has been described in Carrasco *et al.*¹⁶

Results

Product yields from the reaction of sabinene with OH radicals have been measured in the absence of NO_x in the UCC chamber and in the presence of NO_x in the LISA chamber.

Table 1 IBI of the main IR absorption bands, values are given in \log_e

Compound	Main absorption band/ cm^{-1}	IBI/ cm molecule^{-1}	Ref.
Sabinene	2800–3110	$(5.44 \pm 0.15) \times 10^{-17}$	This work
Acetone	1260–1150	$(1.02 \pm 0.02) \times 10^{-17}$	Picquet-Varrault <i>et al.</i> ³²
Formaldehyde	1845–1625	$(1.25 \pm 0.13) \times 10^{-17}$	Klotz <i>et al.</i> ³³
Sabinaketone	1700–1800	$(3.7 \pm 0.4) \times 10^{-17}$	This work

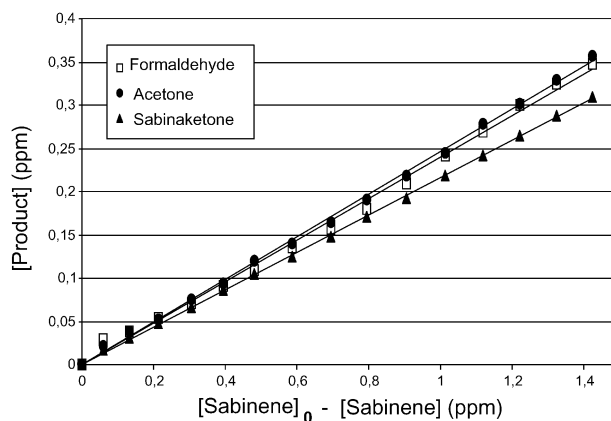


Fig. 1 Formation of acetone, formaldehyde and sabinaketone during a reaction between sabinene and OH (19/11/03 CRAC).

Three primary carbonyl compounds have been observed and quantified, acetone, formaldehyde and sabinaketone. Formation yields were determined by calculating the initial slopes of the plots (see Fig. 1). Uncertainties take in account twice the standard deviation and uncertainties on calibrations. A typical plot of $[\text{product}]$ vs. $-\Delta[\text{sabinene}]$ is given in Fig. 1. The linearity of the plot indicates that the three carbonyl compounds are primary products. As can be seen in Fig. 1, these yield plots are fairly straight lines indicating that the secondary chemistry was negligible under our conditions. Consequently, no correction for secondary reaction was made. Indeed, based on the literature data for OH + sabinene and OH + sabinaketone, HCHO and acetone, the maximum corrections of the measured concentrations for secondary reactions with OH radicals were less than 2% at the highest extent of reaction (about 30% based on the initial sabinene concentration—see Fig. 1), and were neglected. No noticeable difference has been observed between both NO_x conditions. Thus production yields are averaged and compared to previous literature data in Table 2.

Hakola *et al.*⁹ and Arey *et al.*¹⁰ have observed a sabinaketone yield slightly lower than our determination. Nevertheless the three studies are in good accordance considering the overall combined uncertainties. The major outcome of this part of the work was to detect quantitatively sabinaketone by FTIR after its preliminary synthesis and calibration. Indeed, this compound is not commercially available and had been indirectly identified and quantified by Arey *et al.*¹⁰ and Hakola *et al.*⁹ in GC-MS and GC-FID, respectively, assuming a sabinaketone response factor equal to that of a similar compound. Only one previous study (Librando *et al.*¹⁷) reported formaldehyde production yield from the sabinene reaction with OH radicals. They found a higher yield than the one presented in this work. From the experimental details given such a discrepancy is difficult to interpret as it is not clear if secondary chemistry occurred in the Librando *et al.*¹⁷ study. It must also be pointed out that they reported chemical instability and/or photolysis of sabinene under their experimental conditions, while the tests we performed did not show any of these behaviours. The additional formaldehyde could possibly arise from these pathways.

Table 2 Production yields observed in this work and compared with previous literature data

Product	Acetone	Formaldehyde	Sabinaketone	Carbon Balance
181103 CRAC (no NO _x)	0.22 ± 0.05	0.27 ± 0.05	0.23 ± 0.06	0.30 ± 0.07
191103 CRAC (no NO _x)	0.27 ± 0.05	0.23 ± 0.05	0.21 ± 0.06	0.30 ± 0.07
020304 LISA (with NO _x)	0.25 ± 0.05	0.28 ± 0.06	0.19 ± 0.05	0.28 ± 0.07
030304 LISA (with NO _x)	0.21 ± 0.05	0.22 ± 0.04	0.19 ± 0.05	0.26 ± 0.06
Averaged yields (this work)	0.24 ± 0.06	0.25 ± 0.06	0.20 ± 0.06	0.28 ± 0.10
Hakola <i>et al.</i> ⁹	ND	ND	0.17 ± 0.03	0.15 ± 0.03
Arey <i>et al.</i> ¹⁰	ND	ND	0.17	0.15
Reissell <i>et al.</i> ⁸	0.19 ± 0.03	ND	ND	0.06 ± 0.01
Librando <i>et al.</i> ¹⁷	ND	0.61	ND	ND

ND: Not determined

Acetone yield has been previously studied by Reissell *et al.*,⁸ leading to a value $R_{\text{acetone}} = 0.19 \pm 0.03$, which is slightly lower than our determination of $R_{\text{acetone}} = 0.24 \pm 0.06$ but in agreement within the error bars. It must be pointed out that both studies found a primary production of acetone. This shows that acetone is directly arising from the evolution of the radical produced from the initial attack of sabinene and not from the further oxidation of intermediary species. Considering the chemical structure of sabinene, this direct production is not trivial.

Consequently, our study is more exhaustive than previous studies that were focused on the production of one specific compound, acetone or sabinaketone. Nevertheless the carbon balance taking into account the three carbonyl compounds is only equal to 0.28 ± 0.10 and is still highly incomplete. Librando *et al.*¹⁷ reported a 300% molar yield for CO₂ and a 250% molar yield for CO. It is not clear from this article if these yields are primary or secondary but on a carbon balance basis it would represent around 52%. Under our conditions it was not possible to precisely measure these species, because of some strong interferences of the IR absorption of water and already present CO₂. Consequently, it was not possible to confirm these results but such a huge CO and CO₂ production would significantly increase our carbon balance.

Theoretical study

In parallel with the experimental study, we have investigated the potential energy surface (PES) for the OH + sabinene reaction in order to propose a mechanism which can explain the formation of the products experimentally observed. To our knowledge, no theoretical study has been done so far on the mechanism of the oxidation of sabinene by OH radical. In this work, the geometries of the minima and saddle points were fully optimized for the intermediates of the title reaction using quantum chemistry methods. The saddle points are characterized by the existence of only one negative eigenvalue of the Hessian matrix corresponding to an imaginary frequency in the normal mode analysis. We have considered the transition states to be located at the saddle points along the reaction paths. The calculations have been performed at the DFT-B3LYP/6-31G(d,p) level of theory,¹⁸ a method which has already been validated in earlier studies on open-shell systems.^{19–23} As a matter of fact, the overall reaction studied is a doublet open-shell system. For these large systems, this DFT method is a good compromise between reliability and compu-

tational time. For the H-abstraction reactions, calculations have also been performed at the *ab initio* MP2/6-31G(d,p) level of theory. All energies presented in the text and figures are corrected by zero-point energies. No scaling factors have been applied to the frequencies. All these quantum chemical calculations have been performed using the Gaussian 03²⁴ package. The goal of this study is not quantitative but qualitative in order to explain the experimentally observed products.

Geometry of sabinene. The geometric structure of sabinene corresponds to a bicyclic structure, in which a 3-membered and 5-membered ring have a single C–C bond in common. The dihedral angle between these two rings is around 90°.

Initial reactions of sabinene. The oxidation of the sabinene by OH radical can proceed through two main channels: the addition on the double bond C=C of sabinene or the direct abstraction of a hydrogen atom from sabinene by OH.^{25,26} These pathways are complex and involve many intermediary species.

1. Addition of OH to the C=C double bond of sabinene and subsequent reactions

The addition of the OH radical to the double bond of sabinene leads to the adduct ADDa, a primary radical or ADDb, a tertiary radical, depending on the addition site C_a or C_b (see the right-hand side of Fig. 2). Our calculations show that this exothermic addition reaction is barrierless (see the Appendix for discussion about the addition barrier) and largely exothermic by almost 27 kcal mol⁻¹ for the formation of the OH-adduct isomers ADDa and 30 kcal mol⁻¹ for the OH-adduct ADDb.

Both radicals ADDa and ADDb can promptly react with O₂ to form, the peroxy radicals ADDaO₂ and ADDbO₂, respectively. Then, these peroxy radicals react with NO, yielding ADDa(b)O alkoxy radicals. As shown in recent publications,^{26,27} the alkoxy radicals RO* (R = ADDa or ADDb) formed are chemically activated, and can undergo thermalisation or unimolecular reactions, dissociation or isomerisation.

Fate of ADDaO alkoxy radical. As shown in Fig. 3, two unimolecular reaction pathways can possibly occur to ADDaO. β-C–C bond breaking, leading to the hydroxy-sabinenyl radical and formaldehyde through a barrier (TSD1) which lies 5.5 kcal mol⁻¹ above the energy of ADDaO. This low value of

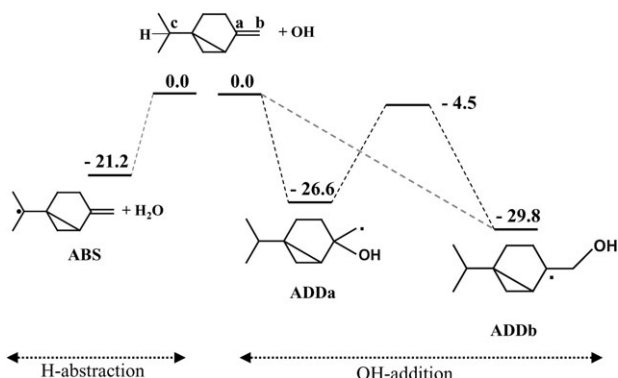


Fig. 2 Schematic molecular structures and energetics for the OH + sabinene initial addition and abstraction reactions from DFT-B3LYP/6-31G(d,p) calculations. The energies are given in kcal mol⁻¹ and include zero-point energy corrections.

the transition state energy is in good agreement with available experimental data for β -hydroxy-alkoxy radicals similar to this one and calculations performed at the same level of theory as in this work.^{19–22} After reaction with O₂, the hydroxy-sabinenyl radical formed will lead to sabinaketone. The other reaction pathway is isomerisation of ADDaO involving a 1,6-H shift of the isopropyl hydrogen atom to the terminal oxygen site of the radical alkoxy, forming the di-hydroxy isopropyl adduct radical *via* a transition state TSI1. The geometry of this transition state is presented in Fig. 4. For a better understanding, the hydrogen atoms are not shown, except for the specific H-atom which is migrating. It can be seen that TSI1 exhibits a 7-membered ring with O \cdots H and C \cdots H distances of 1.35 and 1.40 Å, respectively. This hydrogen shift is associated with a 20 kcal mol⁻¹ barrier height (TSI1) due in part to the constraint of three of the carbon atoms which are common to this ring and the 5-membered ring of the sabinene structure. The large difference between the heights of the two barriers TSI1 and TSD1 (Fig. 3) suggests that the formation of the di-hydroxy isopropyl alkyl radical (DHIR) will have a small probability. If formed, this latter radical can then react with O₂ and NO to give the di-hydroxy isopropyl alkoxy radical which, in turn, undergoes dissociation *via* a barrier of 14 kcal mol⁻¹ height leading finally to acetone.

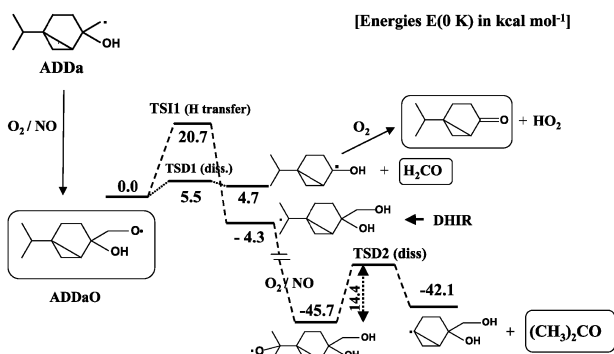


Fig. 3 Energetic diagram of the subsequent reactions of ADDaO from DFT-B3LYP/6-31G(d,p) calculations. The energies are given in kcal mol⁻¹ and include zero-point energy corrections.

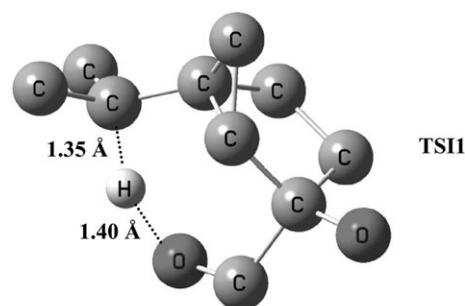


Fig. 4 Molecular structure of the transition state TSI1 showing a 1,6-H atom transfer within the ADDaO carbon structure. The hydrogen atoms are not shown, except for the one which is migrating.

Since, in the presence of NO, the formation of the chemically activated nascent ADDaO* (from DHIR, see Fig. 3) and its subsequent unimolecular reactions could be the first and key steps in the mechanism leading to acetone formation, we have performed statistical kinetic calculations to estimate the probability of isomerisation of the alkoxy radical ADDaO*. These calculations have been performed using the RRKM master equation analysis described in ref. 28 where tunnelling has been taken into account. The results show that isomerisation of ADDaO* through TSI1 is unimportant compared to the dissociation channel leading to sabinaketone. As a consequence, the yield of acetone formed by this pathway is predicted to be unimportant.

Fate of ADDbO alkoxy radical. ADDbO can undergo three dissociation channels as shown in Fig. 5. The first one is a β -C–C dissociation yielding sabinaketone and formaldehyde through a 6.7 kcal mol⁻¹ barrier height (TSD2). The two other pathways involve the opening of the five-membered ring by cleavage of each of the C–C bonds in the α position to the C–O bond. These latter reaction channels have much higher barriers 12.4 (TSC1) and 18.6 kcal mol⁻¹ (TSC2) than the one corresponding to ADDbO dissociation (TSD2). Moreover, they do not play any role in acetone, sabinaketone or formaldehyde formation.

In summary, the two OH-addition channels to sabinene will lead quite easily to sabinaketone and formaldehyde formation,

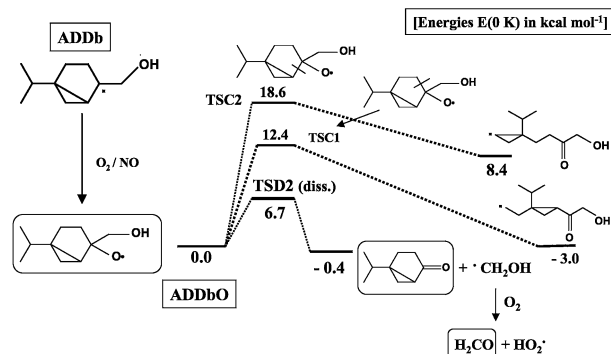


Fig. 5 Energetic diagram of the subsequent reactions of ADDbO from DFT-B3LYP/6-31G(d,p) calculations. The energies are given in kcal mol⁻¹ and include zero-point energy corrections.

but to a low percentage of acetone, not representative of the experimental results which show a primary formation of 20%.

2. Direct H-atom abstraction mechanism

A possibility which could be important in the primary formation of acetone is the direct abstraction by OH of the isopropylidic hydrogen atom of sabinene. In their paper, Kwok and Atkinson²⁵ consider the H-abstraction pathway to be minor when compared to OH-addition, but some measurements have shown that in some cases, it can represent up to 30% of the total rate constant.²⁶ We have therefore explored the PES associated with this possible mechanism. Among the hydrogen atoms of sabinene, the isopropylidic one is the easiest to abstract, since it is linked to a tertiary carbon atom (C_c) (Fig. 2, left). The exothermicity of this abstraction pathway is $-21 \text{ kcal mol}^{-1}$ including the zero-point vibrational (ZPE) correction. An early barrier has been characterized for which the HO \cdot –H distance is equal to 1.81 Å and the C–H bond has lengthened by only 0.05 Å. This transition state lies below the energy of the reactants by 2 kcal mol⁻¹ using the B3LYP/6-31G(d,p) level of theory. Skokov and Wheeler³⁰ have shown that B3LYP/6-31G(d) values are, on average, within a range of 1.6 kcal mol⁻¹ with respect to the experimental energies at most for a set of 6 abstraction reactions and that increasing basis set does not provide better transition state geometries and barriers heights. Another study by Basch and Hoz³¹ also note a good performance for DFT-B3LYP barriers with respect to experiment and high level *ab initio* calculations. We have performed calculations at the *ab initio* PMP2/6-31G(d,p) level of theory and found a barrier of 0.8 kcal mol⁻¹ including ZPE correction. More sophisticated calculations are difficult to perform on this system. Moreover, we cannot *a priori* calculate barrier heights with a sufficient accuracy to allow the prediction of the relative percentage of abstraction with respect to addition. Nevertheless, these low values and the presence of acetone in the products of the experiment lead us to admit that this abstraction reaction can take place. The radical “sabinenyl” called ABS, a product of this abstraction, can undergo addition with molecular oxygen O₂ and the resulting peroxy radical ABSO₂ will react with NO to give ABSO* and NO₂. These steps are described in detail in Fig. 6. The chemically activated nascent ABSO* then undergoes a β–C–C bond breakage leading to acetone. The transition state for this decomposition lies 14.9 kcal mol⁻¹ above ABSO (including the zero-point vibrational correction). This result agrees well with the structure–activity relationship that we proposed in a previous paper²⁰ for activation energies of dissociation reactions of alkoxy radicals. From these results, we can predict that the abstraction channel has to be taken into consideration to explain the acetone formation observed experimentally.

Discussion of the reaction mechanism with and without NO^{27–29}. As a result of our calculations, sabinaketone is mainly formed after OH addition to both sides of the C=C bond of sabinene, involving formation of peroxy radical intermediates RO₂*. In the presence of NO, the RO₂* + NO reactions lead to vibrationally activated alkoxy radicals RO**

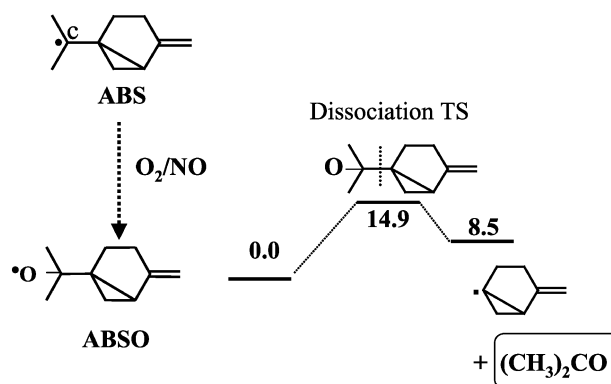
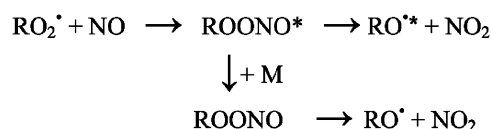
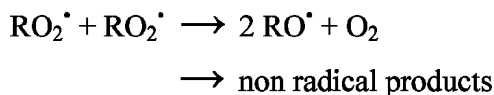


Fig. 6 Energetic diagram of the formation of acetone from the alkyl radical ADD, product of the isopropylidic H-abstraction from the sabinene by the OH radical. The energies are given in kcal mol⁻¹ and include zero-point energy corrections.

and peroxy nitrates:



In the absence of NO, self reactions RO₂* + RO₂* lead to (not activated) alkoxy radicals



The limiting process for yielding acetone in the addition process is the isomerisation transition state (TS1). RRKM-ME calculations have revealed that, even if the alkoxy radical ADDaO is chemically activated, TS1 is too tight and its barrier too high to allow the alkoxy radical to isomerize and therefore yield acetone. Alternatively, both alkoxy radicals ADDa(b)O will easily decompose to give sabinaketone and formaldehyde in the same yield. Alternatively, the alkoxy radical formed from isopropylidic H-atom abstraction from sabinene can decompose easily to give acetone (with or without NO). We can conclude that, in this specific problem, the way by which the alkoxy radicals are formed does not change their reactivity. Some hydroxyalkoxynitrates will also be formed, but in a small quantity.

Conclusion

In this work, parallel experimental and theoretical studies have been undertaken in order to characterize products and propose a degradation mechanism for the gas phase oxidation of sabinene by hydroxyl radicals. Three products have been experimentally characterized and quantified: sabinaketone [(20 ± 6)%], formaldehyde [(25 ± 6)%] and acetone [(24 ± 6)%]. The simultaneous quantification of these compounds is one of the major results of this work. Nevertheless the carbon balance taking into account the three carbonyl compounds is only equal to 0.28 ± 0.10 and is still highly incomplete. Considering the high reactivity of sabinene toward OH³

($k_{\text{OH}} = 1.1 \times 10^{-10} \text{ cm}^3 \text{ molecule}^{-1} \text{ s}^{-1}$), it is very unlikely that the H-atom abstraction from secondary and primary carbons would compete with the considered pathways leading to significant quantities of undetected products. No information on the secondary organic aerosol production was available during this study, but the reactions between terpenes and OH radicals are generally considered³⁴ to be weak aerosol generation pathways. Hence it is also unlikely that the missing carbon would be in the particulate phase. In addition, since one can not observe any significant differences between the results in the presence and in the absence of NO_x , it is also unlikely that a huge hydroxynitrate production could account for the missing pathways.

Considering that (i) no other major chemical functions can be detected from our residual experimental FTIR spectra, (ii) we were not able to precisely quantify CO and CO_2 and (iii) a previous study¹⁷ has proposed a yield of 250 and 300%, respectively, for these compounds, one cannot exclude that the hydroxyalkoxy radical formed after the OH addition may undergo some other processes such as carbon-chain fragmentation which would lead to CO and CO_2 formation. Such drastic decomposition may also explain the additional formaldehyde production. Indeed, the fact that the formaldehyde production yield is slightly higher than the sabinaketone production yield can mean that formaldehyde is not only a co-product of sabinaketone. This fragmentation occurring after opening of the sabinene ring could be an alternative pathway to the acetone production.

The exploration of the different channels of the PES for the reaction using the DFT-B3LYP/6-31G(d,p) quantum method allows us to explain the presence of the three primary products. Two main channels have been explored revealing that sabinaketone and HCHO are formed through the addition of an OH radical to the C=C bond of sabinene. In the presence of NO, some peroxy nitrates are also formed. Alternatively, the H-atom abstraction from the tertiary C-H bond in the $-\text{CH}(\text{CH}_3)_2$ group is predicted to be the most important abstraction site and leads mainly to acetone (plus sabinenyl radical). Quantitative theoretical study is quite impossible, due to the complexity of the reactions, but this qualitative approach can already give new insight into the sabinene + OH reaction.

As stated above, based on the sabinaketone and acetone yields, the OH addition and the H-abstraction pathways only account for 44% of the reaction pathways. The missing channels are thus difficult to predict, considering the complexity of the radicals arising from the ring fragmentation. Additional experiments focused on CO/ CO_2 detection and supplementary calculations would clearly help to clarify this point.

No significant difference has been noted between reactions with and without NO_x . The similar carbonyl productions observed in our study are explained by an efficient peroxy-to-alkoxy conversion in both the presence and absence of NO_x , knowing that the H-abstraction pathway and the OH radical addition to the terminal $=\text{CH}_2$ group pathway mainly lead to tertiary peroxy radicals. The calculations show that the formed alkoxy radicals (vibrationally activated or not) will preferentially decompose by scission of the C-C bond in the β

position with respect to CO^\bullet and give sabinaketone and formaldehyde (OH addition on sabinene) and acetone (H-atom abstraction from sabinene).

This work illustrates the usefulness of quantum calculations in the understanding of the atmospheric chemistry of biogenic compounds. Indeed these species exhibit unusual chemical reactivity most of the time because of their complex structures for which structure activity relationships are often less efficient.

Appendix

Consequence of the long range potential between OH radical and an ethylenic double bond

The existence of a potential energy barrier for an exchange reaction like $\text{A} + \text{BC} \rightarrow \text{AB} + \text{C}$ can be explained by models involving the crossing of two correlation lines between states of reactants and products. Another way to interpret such a behaviour (in fact not really a different way) is to analyze the competition between two processes: the BC bond cleavage which tends to increase the energy and the AB bond forming which favours the energy decrease. This model is the basis of the concept of an intrinsic barrier described by Murdoch.³⁵ Coupled to the exo or endothermicity of the $\text{A} + \text{BC}$ process, this concept of an intrinsic barrier leads to the so called early or late barrier largely used by the chemist invoking the Hammond postulate and by Polanyi to explain the dynamics of these exchange three-atom reactions³⁶

In our case, we deal with an OH addition on a double bond. This process can be compared to an exchange reaction since a single C-O bond is created while a π bond is broken. The dipole moment of an OH radical is rather large (1.76 D). It turns out that when OH is approaching the ethylenic double bond, the attractive long range interaction between this dipole and the electronic doublet of the ethylenic bond dominates over the weakening of this double bond which occurs for much shorter O-C distances. As a matter of fact, neither the C=C distance nor the π C=C bond order vary significantly as long as OH approaches C=C over long distances. Therefore, the domination of this attractive long range potential makes the approach barrierless.

Acknowledgements

J.C.R. and M.T.R. thank IDRIS (CNRS) for computer facilities and F. Caralp for RRKM-master equation calculations. N.C. and J.F.D. thank Dr John Wenger (UCC-CRAC) for simulation chamber facilities. The experimental part of this work have been achieved thanks to the support of EURO-CHAMP, an Integrated Infrastructure Initiative of the 6th framework European program.

References

- 1 A. Guenther, C. N. Hewitt, D. Erickson, R. Fall, C. Geron, T. Graedel, P. Harley, L. Klinger, M. Lerdau, W. A. McKay, T. Pierce, B. Scholes, R. Steinbrecher, R. Tallamraju, J. Taylor and P. Zimmerman, *J. Geophys. Res.*, 1995, **100**, 8873.
- 2 A. Guenther, C. Geron, T. Pierce, B. Lamb, P. Harley and R. Fall, *Atmos. Environ.*, 2000, **34**, 2205.

- 3 R. Atkinson, S. M. Aschmann and J. Arey, *Atmos. Environ., Part A*, 1990, **24**, 2647.
- 4 L. Tollsten and M. Müller, *Phytochemistry*, 1996, **43**, 759.
- 5 S. Owen, C. Boissard, R. A. Street, S. C. Duckham, O. Csiky and C. N. Hewitt, *Atmos. Environ.*, 1997, **31**, 101.
- 6 R. A. Street, S. Owen, S. C. Duckham, C. Boissard and C. N. Hewitt, *Atmos. Environ.*, 1997, **31**, 89.
- 7 H. Hakola, J. Rinne and T. Laurila, *Atmos. Environ.*, 1998, **32**, 1825.
- 8 A. Reissell, C. Harry, S. M. Aschmann, R. Atkinson and J. Arey, *J. Geophys. Res.*, 1999, **104**, 13869.
- 9 H. Hakola, J. Arey, S. M. Aschmann and R. Atkinson, *J. Atmos. Chem.*, 1994, **18**, 75.
- 10 J. Arey, R. Atkinson and S. M. Aschmann, *J. Geophys. Res.*, 1990, **95**, 18–539.
- 11 L. Jaeglé, D. J. Jacob, W. H. Brune and P. O. Wennberg, *Atmos. Environ.*, 2001, **35**, 469.
- 12 D. Jacob, B. D. Field, E. M. Jin, I. Bey, Q. Li, J. A. Logan, R. M. Yantosca and H. B. Singh, *J. Geophys. Res.*, 2002, **107**(D10), 4100.
- 13 J. F. Doussin, D. Ritz, R. Durand-Jolibois, A. Monod and P. Carlier, *Analysis*, 1997, **25**, 236.
- 14 L. Thuener, P. Bardini, G. J. Rea and J. Wenger, *J. Phys. Chem. A*, 2004, **108**, 11019.
- 15 W. D. Taylor, T. D. Allston, M. J. Moscato, G. B. Fazekas, R. Kozlowski and G. A. Takacs, *Int. J. Chem. Kinet.*, 1980, **12**, 231.
- 16 N. Carrasco, J. F. Doussin, B. Picquet-Varrault and P. Carlier, *Atmos. Environ.*, 2006, **40**, 2011.
- 17 V. Librando and G. Tringali, *J. Environ. Management*, 2005, **75**, 275.
- 18 A. D. Becke, *J. Chem. Phys.*, 1993, **98**, 5648.
- 19 F. Caralp, P. Devolder, C. Fittschen, N. Gomez, H. Hippler, R. Méreau, M. T. Rayez, F. Striebel and B. Viskolcz, *Phys. Chem. Chem. Phys.*, 1999, **1**, 2935.
- 20 R. Méreau, M. T. Rayez, F. Caralp and J. C. Rayez, *Phys. Chem. Chem. Phys.*, 2000, **2**, 3765.
- 21 R. Méreau, M. T. Rayez, J. C. Rayez and F. Caralp, *Phys. Chem. Chem. Phys.*, 2003, **5**, 4828.
- 22 R. Méreau, M. T. Rayez, F. Caralp and J. C. Rayez, *Phys. Chem. Chem. Phys.*, 2000, **2**, 1919.
- 23 L. Vereecken and J. Peeters, *J. Phys. Chem. A*, 2000, **104**, 11140.
- 24 M. J. Frisch, G. W. Trucks, H. B. Schlegel, G. E. Scuseria, M. A. Robb, J. R. Cheeseman, J. A. Montgomery Jr, T. Vreven, K. N. Kudin, J. C. Burant, J. M. Millam, S. S. Iyengar, J. Tomasi, V. Barone, B. Mennucci, M. Cossi, G. Scalmani, N. Rega, G. A. Petersson, H. Nakatsuji, M. Hada, M. Ehara, K. Toyota, R. Fukuda, J. Hasegawa, M. Ishida, T. Nakajima, Y. Honda, O. Kitao, H. Nakai, M. Klene, X. Li, J. E. Knox, H. P. Hratchian, J. B. Cross, V. Bakken, C. Adamo, J. Jaramillo, R. Gomperts, R. E. Stratmann, O. Yazyev, A. J. Austin, R. Cammi, C. Pomelli, J. W. Ochterski, P. Y. Ayala, K. Morokuma, G. A. Voth, P. Salvador, J. J. Dannenberg, V. G. Zakrzewski, S. Dapprich, A. D. Daniels, M. C. Strain, O. Farkas, D. K. Malick, A. D. Rabuck, K. Raghavachari, J. B. Foresman, J. V. Ortiz, Q. Cui, A. G. Baboul, S. Clifford, J. Cioslowski, B. B. Stefanov, G. Liu, A. Liashenko, P. Piskorz, I. Komaromi, R. L. Martin, D. J. Fox, T. Keith, M. A. Al-Laham, C. Y. Peng, A. Nanayakkara, M. Challacombe, P. M. W. Gill, B. Johnson, W. Chen, M. W. Wong, C. Gonzalez and J. A. Pople, *GAUSSIAN 03 (Revision C.02)*, Gaussian, Inc., Wallingford CT, 2004.
- 25 E. S. C. Kwok and R. Atkinson, *Atmos. Environ.*, 1995, **29**(14), 1685.
- 26 J. Peeters, S. Vandenberk, E. Piessens and V. Pultau, *Chemosphere*, 1999, **38**(6), 1189.
- 27 J. J. Orlando, G. S. Tyndall, L. Vereecken and J. Peeters, *J. Phys. Chem. A*, 2000, **104**, 11578.
- 28 J. J. Orlando, G. S. Tyndall and T. J. Wallington, *Chem. Rev.*, 2003, **103**, 4657, and references therein.
- 29 F. Caralp, W. Forst and M. T. Rayez, *Phys. Chem. Chem. Phys.*, 2003, **5**, 476.
- 30 S. Skokov and R. A. Wheeler, *Chem. Phys. Lett.*, 1997, **271**, 251.
- 31 H. Basch and S. Hoz, *J. Phys. Chem. A*, 1997, **101**, 4416.
- 32 B. Picquet-Varrault, J. F. Doussin, R. Durand-Jolibois and P. Carlier, *Environ. Sci. Technol.*, 2002, **36**, 4081.
- 33 B. Klotz, I. Barnes and T. Imamura, *Phys. Chem. Chem. Phys.*, 2004, **8**, 1725.
- 34 T. Hoffman, J. R. Odum, F. Bowman, D. Collins, D. Klockow, R. C. Flagan and J. H. Seinfeld, *J. Atmos. Chem.*, 1997, **26**, 189.
- 35 J. R. Murdoch, *J. Am. Chem. Soc.*, 1983, **105**, 2159.
- 36 J. C. Polanyi, *Acc. Chem. Res.*, 1972, **5**, 161.